

1 **Heterochromatin protein 1 α mediates development and**
2 **aggressiveness of neuroendocrine prostate cancer**

3 **Authors:** Xinpei Ci^{1,2}, Jun Hao^{1,2}, Xin Dong², Stephen Y. Choi^{1,2}, Hui Xue², Rebecca Wu²,
4 Sifeng Qu^{1,2}, Peter W. Gout², Fang Zhang², Anne M. Haeger¹, Ladan Fazli¹, Francesco
5 Crea³, Christopher J. Ong¹, Amina Zoubeidi¹, Housheng H. He^{4,5}, Martin E. Gleave¹, Colin C.
6 Collins¹, Dong Lin^{1,2,*}, Yuzhuo Wang^{1,2,*}

7 **Author affiliation:** ¹Vancouver Prostate Centre, Department of Urologic Sciences,
8 University of British Columbia, Vancouver, BC, Canada.

9 ²Department of Experimental Therapeutics, BC Cancer, Vancouver, BC, Canada.

10 ³School of Life, Health & Chemical Sciences, The Open University, Walton Hall, Milton
11 Keynes, MK7 6AA, United Kingdom.

12 ⁴Princess Margaret Cancer Center, University Health Network, Toronto, Ontario, Canada.

13 ⁵Department of Medical Biophysics, University of Toronto, Toronto, Ontario, Canada.

14 **Running title:** Heterochromatin gene signature unveils HP1 α mediating NEPC

15 **Key words:** Neuroendocrine prostate cancer, HP1 α , Transdifferentiation, PDX

16 **Conflict of Interest:** The authors have no conflicts of interest to disclose.

17 **Word Count (Main text):** 5069

18 **Number of Figures:** 6

19 *** Corresponding author:**

20 Yuzhuo Wang
21 Vancouver Prostate Centre
22 Department of Urologic Sciences, University of British Columbia
23 2660 Oak Street, Vancouver,
24 BC V6H 3Z6, Canada
25 Phone: 604-675-8013, email: ywang@bccrc.ca

26

27 Dong Lin
28 Vancouver Prostate Centre
29 Department of Urologic Sciences, University of British Columbia
30 2660 Oak Street, Vancouver
31 BC V6H3Z6, Canada
32 Phone: 604-675-7013, email: dlin@prostatecentre.com

33

34 **ABSTRACT (230 WORDS)**

35 Neuroendocrine prostate cancer (NEPC) is a lethal subtype of prostate cancer (PCa)
36 arising mostly from adenocarcinoma via NE transdifferentiation following androgen
37 deprivation therapy. Mechanisms contributing to both NEPC development and its
38 aggressiveness remain elusive. In light of the fact that hyperchromatic nuclei are a
39 distinguishing histopathological feature of NEPC, we utilized transcriptomic analyses of our
40 patient-derived xenograft (PDX) models, multiple clinical cohorts, and genetically engineered
41 mouse models to identify 36 heterochromatin-related genes that are significantly enriched in
42 NEPC. Longitudinal analysis using our unique, first-in-field PDX model of adenocarcinoma-
43 to-NEPC transdifferentiation revealed that, among those 36 heterochromatin-related genes,
44 heterochromatin protein 1 α (HP1 α) expression increased early and steadily during NEPC
45 development and remained elevated in the developed NEPC tumor. Its elevated expression
46 was further confirmed in multiple PDX and clinical NEPC samples. *HP1 α* knockdown in the
47 NCI-H660 NEPC cell line inhibited proliferation, ablated colony formation, and induced
48 apoptotic cell death, ultimately leading to tumor growth arrest. Its ectopic expression
49 significantly promoted NE transdifferentiation in adenocarcinoma cells subjected to androgen
50 deprivation treatment. Mechanistically, HP1 α reduced expression of androgen receptor (AR)
51 and RE1 silencing transcription factor (REST) and enriched the repressive trimethylated
52 histone H3 at Lys9 (H3K9me3) mark on their respective gene promoters. These
53 observations indicate a novel mechanism underlying NEPC development mediated by
54 abnormally expressed heterochromatin genes, with HP1 α as an early functional mediator
55 and a potential therapeutic target for NEPC prevention and management.

56 **Statement of Significance**

57 Heterochromatin proteins play a fundamental role in neuroendocrine prostate cancer,
58 illuminating new therapeutic targets for this aggressive disease.

59 INTRODUCTION

60 Neuroendocrine prostate cancer (NEPC) has become a clinical challenge in the
61 management of castration resistant prostate cancer (CRPC). While *de novo* cases are rare,
62 NEPC as a special subtype of CRPC (~10-20%) is thought to occur via NE
63 transdifferentiation of prostate adenocarcinomas in response to androgen deprivation
64 treatment (ADT), resisting dependence on AR signaling as an adaptive response. As next-
65 generation AR pathway inhibitors (ARPI) such as enzalutamide and abiraterone have made
66 substantial improvements in managing CRPC adenocarcinomas in recent years (1), it is
67 expected that the incidence of NEPC will further increase (2). Unfortunately, the overall
68 median survival of NEPC with small cell feature is less than one year, primarily due to its
69 aggressiveness and limited available treatment options (3). As such, a better understanding
70 of the mechanisms underlying NEPC development remains much needed in order to
71 develop more effective therapeutics.

72 One distinct histopathological feature of NEPC cells is the frequent manifestation of
73 hyperchromatic nuclei with finely dispersed chromatin and inconspicuous nucleoli, a
74 phenomenon known as “salt and pepper” chromatin (3,4). This is in contrast to prostatic
75 adenocarcinoma cells, which tend to have enlarged nuclei with prominent nucleoli (3,4). This
76 special hematoxylin-staining characteristic suggests a distinct NEPC heterochromatin
77 pattern (5). Heterochromatin is a condensed and transcriptionally inert chromosome
78 conformation, regulated epigenetically by precise and dedicated machineries (6,7). Multiple
79 studies have demonstrated that epigenetic regulation is one major mechanism underlying

80 NEPC development (8-11). An NEPC-specific heterochromatin gene signature can thus
81 shed light to help better understand the disease and identify novel therapeutic targets.
82 Another distinct feature of NEPC is the lineage alteration associated with a decrease or loss
83 of crucial adenocarcinoma lineage-specific transcription factors, AR, FOXA1 and REST (12-
84 15). This leads to the repression of AR-regulated genes (e.g. prostate-specific antigen (PSA))
85 and gain of neuroendocrine markers (e.g. neural cell adhesion molecule 1 (NCAM1/CD56),
86 neuronal-specific enolase (NSE), chromogranin A (CHGA), and synaptophysin (SYP)) (12-
87 14). While recent studies have reported that EZH2 inhibits *AR* expression and *SRRM4*
88 mediates *REST* splicing (8,16), the mechanisms underlying the constant transcriptional
89 suppression of *AR* and *REST* are still not well understood.

90 One of the major hurdles in studying NEPC is the lack of clinically relevant models,
91 but substantial progress has been achieved recently in modeling NEPC development.
92 Employing genetically engineered mouse (GEM) models, ectopic gain of *N-myc* and
93 concomitant loss of *Rb1* and *Tp53* have both been demonstrated to induce *de novo* NEPC-
94 like tumors (8,11). Potent ADT using abiraterone in *Tp53/Pten* double deficient mice also
95 promoted overt NE transdifferentiation of luminal adenocarcinoma cells (17). Employing
96 engineered human primary cells or cell lines, *N-myc*, *SOX2*, *BRN2*, and *SRRM4*
97 overexpression have all been shown to promote NE transdifferentiation (16,18-20). Our
98 laboratory has established over 45 high-fidelity patient-derived xenograft (PDX) models of
99 PCa including 5 NEPCs (www.livingtumorlab.ca) (21). Among them, LTL331/331R is the first-
100 in-field and unique PDX model of adenocarcinoma-to-NEPC transdifferentiation. Upon host
101 castration, the primary adenocarcinoma (LTL331) initially regresses but relapses within few

102 months as typical NEPC (LTL331R) (21). Importantly, the whole transdifferentiation process
103 observed in the LTL331/331R model is predictive of disease progression and is fully
104 recapitulated in the donor patient (22), suggesting a strong clinical relevance. Because an
105 overwhelming majority of expressed genes accounting for the NE phenotype in terminal
106 NEPC may obscure the real drivers of disease progression required at earlier stages, we
107 focused on identifying the early changes induced by ADT before NEPC is fully developed,
108 with an additional secondary criterion that these changes persist into terminal NEPC. To this
109 end, we developed a time series of the LTL331 model, for which samples were harvested at
110 multiple points during the transition period following host castration in order to monitor the
111 entire transdifferentiation process and discover potential drivers with early expression
112 changes (22).

113 In this study, we identified a heterochromatin molecular signature that is commonly
114 upregulated in NEPC. Among the signature genes, we discovered that the upregulation of
115 HP1 α (encoded by *CBX5*), a gene prominently associated with constitutive heterochromatin
116 and mediating concomitant gene silencing, was an early event in our LTL331/331R NE
117 transdifferentiation model. HP1 α expression was increased within weeks following castration
118 but before emergence of NE genes, gradually reaching its highest level in terminally
119 developed NEPC. HP1 α is also widely expressed in clinical samples of NEPC. We show that
120 HP1 α is essential for NEPC cell proliferation, survival, and tumor growth, and its elevated
121 expression promotes ADT-driven NE-differentiation in prostatic adenocarcinoma cells. *HP1 α*
122 ectopic expression reduces expression of AR and REST, two crucial transcription factors

123 silenced in NEPC, and enriches the repressive histone mark H3K9me3 on their respective
124 gene promoters.

125 MATERIAL AND METHODS

126 Patient-derived xenografts and clinical datasets

127 All PDX tumor lines were grafted in NSG mice as previously described (21). This
128 study followed the ethical guidelines stated in Declaration of Helsinki, specimens were
129 obtained from patients with their informed written consent form following a protocol (#H09-
130 01628) approved by the Institutional Review Board of the University of British Columbia
131 (UBC). Animal studies under the protocol # A17-0165 were approved by UBC Animal Care
132 and Use Committee. The LTL331 castrated tissues and the NEPC-relapsed LTL331R
133 tissues were harvested at different time points after host castration (22). Transcriptomic
134 analysis for all PDX tumors, with the exception of the LTL331-331R castration time-series
135 samples, was performed using GE 8x60K microarray, as previously described (21).
136 Transcriptomic analysis of the LTL331-331R time-series was done using RNA-sequencing
137 data.

138 The clinical cohorts used in this study are as follows: RNA-seq data for the *Beltran et*
139 *al.* 2011 cohort (30 adenocarcinomas, 6 NEPCs) was from Weill Medical College of Cornell
140 University (23); RNA-Seq data for the *Beltran et al.* 2016 (34 CRPC-adenocarcinomas, 15
141 NEPCs) the *Grasso et al.* 2012 (31 CRPC-adenocarcinomas, 4 NEPCs), and the *Kumar et*
142 *al.* 2016 (149 CRPC-adenocarcinomas) cohorts were accessed through the cBioPortal
143 (10,24-26); microarray data for the *Varambally et al.* 2015 cohort (6 CRPC-
144 adenocarcinomas) was accessed from the Gene Expression Omnibus (GEO) database
145 (GSE3325) (27).

146

147 **Human prostate cancer specimens**

148 PCa specimens were obtained from the Vancouver Prostate Centre Tissue Bank
149 (103 hormone naive primary prostatic adenocarcinomas, 120 CRPC-adenocarcinomas, 8
150 NEPCs). This study followed the ethical guidelines stated in Declaration of Helsinki,
151 specimens were obtained from patients with their informed written consent form following a
152 protocol (#H09-01628) approved by the Institutional Review Board of the University of British
153 Columbia (UBC). Tissue microarrays of duplicate 1 mm cores were constructed manually
154 (Beecher Instruments, MD, USA). NEPC specimens are histologically either small cell
155 carcinoma or large cell neuroendocrine carcinoma with low or negative AR expression and
156 positive CHGA expression as determined by IHC staining.

157

158 **Cell line culture and reagents**

159 NCI-H660 and 293T cells were obtained from ATCC. Cells were authenticated with
160 fingerprinting method at Fred Hutchinson Cancer Research Centre (Seattle, USA).
161 Mycoplasma testing was routinely performed at the Vancouver Prostate Centre. NCI-H660
162 cells was cultured in RPMI-1640 medium (Hyclone) with supplements as follows: 5% FBS
163 (GIBCO), 10 nM beta-estradiol (Sigma), 10 nM Hydrocortisone (Sigma), 1% Insulin-
164 Transferrin-Selenium (Thermo Fisher). V16D (20) cells were maintained in RPMI-1640
165 containing 10% FBS. 293T was kept in DMEM (Hyclone) with 5% FBS. For *in vitro* NE

166 phenotype induction in V16D cells, cells were starved with phenol-red free RPMI-1640
167 (GIBCO) containing 10% Charcoal-Stripped Serum (CSS) (GIBCO) for 24 hours, then
168 cultured in the same media or with the addition of 10 μ M enzalutamide (Haoyuan
169 Chemexpress) for another 14 days (20).

170

171 **Bioinformatics analysis**

172 As previously described, Gene Set Enrichment Analysis (GSEA)
173 (<http://software.broadinstitute.org/gsea/index.jsp>) was used in this study to determine
174 whether a defined set of genes show significant, concordant differences between two
175 biological phenotypes (e.g. PCa adenocarcinoma vs. NEPC) or two sample groups (e.g. shC
176 vs. KD) (28). All GSEA analyses in this study used whole transcriptomic data without
177 expression level cut-off as expression datasets. Normalized values were used for profiling
178 data from PDX tissues, H660 and V16D stable cell lines, and the three NEPC mouse models
179 (GSE90891, GSE92721, GSE86532); raw read numbers was used for RNA-seq data from
180 the *Beltran et al.* 2011 cohort; pre-ranked gene list based on p -value from lowest to highest
181 was used for the *Beltran et al.* 2016 cohort (8,10,11,17,21,23). Unbiased analysis was
182 performed using the latest MSigDB database for each collection (29). Phenotype
183 permutation was applied when the sample size grouped in one phenotype was more than
184 five. Otherwise, gene set permutation was employed. False discovery rate (FDR) q values
185 were calculated using 1000 permutations, a geneset was considered significantly enriched if
186 its normalized enrichment score (NES) has an FDR q below 0.25.

187 Ingenuity pathway analysis (IPA) was performed as previously described (20).
188 Differentially expressed genes were selected based on the criteria that their standard
189 deviation between samples of one group (e.g. three HP1 α knockdown lines) is below 0.5
190 and their student's *t*-test *p*-value between groups (e.g. shC vs. KD) is below 0.05.

191 For the NE scores and the heterochromatin score, the weight for each gene in the
192 score list was first calculated by taking the log₂ of the *p*-value of all genes and multiplying it
193 by the sign of the fold change. The weight for each gene in *Lee et al.* 2016 was obtained
194 directly from their study. The *p*-values for the genes contributing to heterochromatin score
195 was calculated by comparing NEPC PDXs with all other adenocarcinoma PDXs with the
196 Student's *t*-test. A score was then assigned to each sample by multiplying the weight with
197 the normalized RNA expression value, adding all values for each gene, log-transforming the
198 absolute value of the sum value, and multiplying the sign of the sum value (10,11,18).

199 The heatmap was constructed using the Gplots and heatmap.2 packages in R.
200 Hierarchical clustering was used to determine sample similarity.

201

202 **Statistical analysis and data representation**

203 Statistical analysis was done using the Graphpad Prism software. The Student's *t*-
204 test was used to analyze statistical significance between groups in discrete measurements
205 while two-way ANOVA was used for continuous measurements. The Kaplan-Meier method
206 was used to estimate curves for relapse-free survival, and comparisons were made using

207 the log-rank test. Pearson correlation (with 95% confidence intervals) was used to measure
208 the linear correlation between two variables. Any differences with p -values lower than 0.05 is
209 regarded as statistically significant, with $*p < 0.05$, $**p < 0.01$, $***p < 0.001$. Graphs show pooled
210 data with error bars representing standard error of the mean (SEM) obtained from at least
211 three replicates and standard deviation (SD) of values from clinical samples. Lines in scatter
212 plots represent the median value of measurements from multiple samples and mean with 95%
213 confidence interval (CI) for scores from multiple samples. Box plot with whiskers showing 5-
214 95% percentile values was used to represent analysis of IHC scores.

215

216 **Accession numbers**

217 All PDX microarray profiles are available at www.livingtumorlab.ca, and accessible under the
218 accession number GSE41193 in the GEO database. RNA-seq profiles for the LTL331/331R
219 castration time-series have been deposited to the European Nucleotide Archive and are
220 available under the accession number ENA: PRJEB9660. Microarray profiles for cell lines
221 are deposited (GSE105033).

222 RESULTS

223 NEPC has a distinctive heterochromatin gene signature

224 To determine if a specific gene expression program contributes to the
225 hyperchromatic histological feature of NEPC cells, we first performed an unbiased gene set
226 enrichment analysis (GSEA) using our latest PDX collection and two NEPC clinical cohorts.
227 Transcriptomic profiles from our high-fidelity PDX models (18 adenocarcinomas vs. 4
228 NEPCs), the *Beltran*, et al. 2011 cohort (30 adenocarcinomas vs. 6 NEPCs), and the *Beltran*,
229 et al. 2016 cohort (34 CRPC-adenocarcinomas vs. 15 NEPCs) (10,21,23) all demonstrate
230 that heterochromatin-associated genes are significantly enriched in NEPC compared to
231 adenocarcinoma (Fig. 1A-1C, S1A). We further analyzed three GEM models mimicking the
232 development of NEPC. Interestingly, heterochromatin-associated genes are also significantly
233 enriched as long as NE differentiation occurs, driven by either *Pten/Rb* double knockout
234 (DKO) or *Pten/Rb/Tp53* triple knockout (TKO), *Pten/Tp53* knockout with potent ADT, or *N-*
235 *Myc* overexpression (Fig. 1D-1F) (8,11,17).

236 To further decipher the genes contributing to the heterochromatin feature of NEPC,
237 we analyzed the leading edge genes derived from the GSEA of PDX and clinical NEPC
238 samples (Fig. 1A-1C). Since the NEPCs in our PDX collection are all typical neuroendocrine
239 carcinomas without mixed adenocarcinoma tissues, the upregulated genes identified in the
240 NEPC PDXs and validated in the clinical cohorts can be considered heterochromatin
241 signature genes. In addition, three polycomb-group (PcG) genes, *EZH2*, *RBBP4* and *RBBP7*,
242 are also included in this gene signature as their upregulated expression in NEPC have been

243 previously reported (9,23). They have also been reported to play important roles in
244 heterochromatin formation (7), but are omitted from the GSEA geneset (GO:0000792)
245 containing other PcG members. As such, 36 genes were identified and selected to form a
246 heterochromatin gene panel, which could successfully distinguish NEPC from
247 adenocarcinoma through hierarchical clustering similar to two reported NE score gene
248 panels (Fig. 1G, S1B-S1E) (10,18). From this heterochromatin gene panel, a weighted score
249 was calculated for each sample in the PDX and clinical cohorts following a similar strategy
250 utilized in recent studies (10,11,18). Notably, similar to NEPC samples having a distinctly
251 higher NE score compared to adenocarcinomas, NEPC samples also have a significantly
252 higher heterochromatin score compared to adenocarcinoma (Fig. 1H). Importantly, the
253 heterogeneity among PDX samples is much smaller than that observed in any clinical
254 cohorts regardless of the scoring system employed, further demonstrating that our PDX
255 collection both clearly reflects the clinical features of NEPC and adenocarcinoma and
256 provide a distinct system to study PCa subtypes. Together, these analyses indicate that a
257 heterochromatin-related gene expression signature is a unique feature of NEPC tumors.

258

259 **Expression of heterochromatin protein 1 α (HP1 α) is upregulated early and steadily**
260 **during NEPC development**

261 Inspired by the critical functional role of heterochromatin structure in modulating cell
262 behavior and gene expression (6,7), we hypothesized that these NEPC-specific
263 heterochromatin signature genes could contribute to NEPC development. As such, we

264 attempted to identify a potential NEPC driver gene from our 36 heterochromatin signature
265 genes. In addition to a final upregulation in terminal NEPC, expression of the candidate
266 driver gene would also be increased early prior to full NEPC development. We thus analyzed
267 the RNA-seq profile of the LTL331/331R NE-transdifferentiation model with samples from
268 castration-induced dormant time points prior to full NEPC relapse (21,22). Ranked by the
269 gene expression difference between pre- and post-castration samples, elevated expression
270 of *HP1α* was found to be an early and dramatic event occurring upon host castration.
271 Conversely, expression of other genes that have been reported to be associated with NEPC
272 such as *EZH2* and *CBX2* (9,23) were only upregulated in the fully developed NEPC sample
273 (LTL331R) (Fig. 2A). Interestingly, we also noticed that *Hp1α* expression gradually increased
274 as the NE phenotype progressed from partial to more dominantly overt in the *Pten/Tp53*
275 CRPC mouse model (Fig. S2A), lending further support that elevated *HP1α* expression is an
276 early event in NEPC development.

277 To validate our findings, we performed quantitative RT-PCR (qRT-PCR) to detect
278 *HP1α* expression at the mRNA level and IHC staining and Western blotting to detect HP1α
279 expression at the protein level in our PDX collection. Both the mRNA and protein levels of
280 HP1α are significantly increased in NEPC PDXs (Fig. 2B-2D, S2B). Furthermore, we
281 confirmed HP1α expression in the LTL331/331R castration time-series samples. Consistent
282 with the RNA-seq data, both the mRNA and protein expression of HP1α increased upon host
283 castration, with increased mRNA observed as early as 1 week post-castration and elevated
284 protein expression observed 3 weeks post-castration (Fig. 2E-2G). Taken together, these

285 data demonstrate that elevated expression of HP1 α is an early and consistent event
286 throughout NEPC development and could be a potential driver of NEPC.

287

288 **HP1 α expression is upregulated in clinical NEPC samples and correlates with poor**
289 **prognosis**

290 To determine the clinical relevance of elevated HP1 α expression in NEPC, we
291 analyzed RNA expression profiles from three individual clinical cohorts containing NEPC
292 samples. In the *Beltran* et al. 2011 cohort, *HP1 α* expression was about 4 times higher in
293 NEPCs (n=6) compared to adenocarcinomas (n=30) (Fig. 3A) (23). In the *Beltran* et al. 2016
294 cohort, *HP1 α* expression was also significantly upregulated in NEPCs (n=15) compared to
295 CRPC adenocarcinoma samples (n=34) by around two folds (Fig. 3B) (10). In another cohort
296 consisting of 35 metastatic CRPC samples, 4 samples with NEPC features expressed
297 significantly higher *HP1 α* mRNA than other typical adenocarcinomas (Fig. 3C) (24). To
298 better understand the relationship between HP1 α expression and the NEPC phenotype at a
299 protein level, we performed IHC for HP1 α with the Vancouver Prostate Centre (VPC) clinical
300 PCa tissue microarrays (TMAs) containing 103 primary adenocarcinomas, 120 CRPC
301 adenocarcinomas and 8 typical NEPC samples. Consistent with its mRNA level, HP1 α
302 protein was significantly overexpressed in NEPCs (mean=2.45) compared to primary
303 adenocarcinomas (mean=1.66, $p=0.011$) and CRPC adenocarcinomas (mean=1.60,
304 $p=0.014$) (Fig. 3D, 3E). These data together demonstrate that HP1 α is highly expressed in
305 NEPC.

306 While HP1 α is dramatically upregulated in NEPC, we also noticed that some
307 adenocarcinomas also expressed higher levels of HP1 α than others (Fig. 3D). We then
308 investigated whether the expression of HP1 α is associated with poor patient prognosis, thus
309 possibly being a pre-disposing factor to poor outcome. Among the 103 primary
310 adenocarcinoma samples in the VPC cohort, there were 37 samples with clinical follow-up
311 information. Kaplan-Meier analysis showed that patients with high expression of HP1 α (IHC
312 score \geq 2) had a significantly shorter disease-free survival time (HR=4.627, p =0.0074) than
313 low HP1 α -expressing patients (IHC score <2) (Fig. 3F). For CRPC patients, the group with
314 high expression of *HP1 α* (top 1/3) had a significantly shorter overall survival time after the
315 first hormonal therapy (HR=2.961, p =0.021), implying that HP1 α positively correlates with
316 poor prognosis upon hormonal therapy (Fig. 3G). Overall, these analyses indicate that
317 increased expression of HP1 α is a poor prognostic factor in advanced PCa.

318

319 ***HP1 α* knockdown inhibits NEPC cell proliferation and induces apoptosis, leading to**
320 **tumor growth arrest**

321 Considering that HP1 α is significantly upregulated in NEPC, we proceeded to
322 investigate its function in NEPC cells. NCI-H660 is a unique and typical NEPC cell line (30).
323 Consistent with the high HP1 α expression observed in clinical NEPC samples, HP1 α is also
324 expressed at the highest level in H660 cells compared to seven other PCa cell lines at both
325 RNA and protein levels (Fig. S3A). We thus constructed stable H660 cell lines with *HP1 α*
326 knocked down using lentiviral-delivered shRNAs (Fig. 4A). Upon *HP1 α* knockdown, the

327 overall proliferation of H660 cells was significantly inhibited, as evaluated by both crystal
328 violet staining and cell counting (Fig. 4B, S3B). We further performed colony formation
329 assays to evaluate the reproductive and survival ability of single cells. Remarkably, *HP1 α*
330 knockdown was able to ablate the colony formation ability of H660 cells (Fig. 4C). We then
331 proceeded to analyze in greater detail the potential cellular mechanisms underlying the
332 attenuation of cell growth mediated by *HP1 α* knockdown. An EdU incorporation assay
333 showed that knockdown of *HP1 α* led to a significant reduction of EdU-positive, DNA
334 synthesis-active cells (Fig. 4D). Furthermore, an apoptosis assay and FACS analysis
335 indicated that *HP1 α* knockdown also promoted cell early-apoptosis and final death (Fig. 4E,
336 4F). Molecularly, the apoptosis markers cleaved-caspase 3 and cleaved-PARP1 were both
337 upregulated in knockdown cells (Fig. 4G); multiple machineries involved in DNA damage
338 repair and cell cycle progression were also impaired in *HP1 α* knockdown cells as
339 determined by GSEA and ingenuity pathway analysis (IPA) from stable cell line
340 transcriptomic profiles (Fig. 4H, S3C, S3D). Thus, *HP1 α* depletion inhibited NEPC cell
341 proliferation and induced apoptosis *in vitro*.

342 We then assessed the functional impact of *HP1 α* knockdown on tumor growth *in vivo*.
343 Compared to control H660 cells, xenograft tumor growth of the KD2 stable cell line with 70%
344 *HP1 α* knockdown (Fig. 4A, S3E) was observed to be dramatically inhibited and much slower,
345 as determined by continuous tumor volume measurements and final fresh tumor weights
346 (Fig. 4I, 4J). The other two stable lines (KD1, KD3) with 80%~95% *HP1 α* knockdown were
347 not able to generate sufficient cell numbers for *in vivo* tumor formation assays. Taken

348 together, the *in vitro* and *in vivo* studies establish that *HP1α* knockdown could both inhibit
349 NEPC cell proliferation and induce apoptosis, leading to NEPC tumor growth arrest.

350

351 **HP1α promotes NE transdifferentiation of prostatic adenocarcinoma cells following**
352 **ADT**

353 Since *HP1α* was identified as a potential early driver of NEPC development following
354 hormone therapy, we further investigated whether *HP1α* could enhance NE phenotype in
355 ADT-induced NE differentiation of adenocarcinoma cells similar to our LTL331/331R NE-
356 transdifferentiation PDX model. We used V16D cells, a LNCaP-derived CRPC cell line (20),
357 to construct stable cell lines with *HP1α* ectopic expression (Fig. 5A). Upon ADT using
358 charcoal-stripped serum (CSS) or enzalutamide (EnZ) treatment for 14 days, both control
359 and *HP1α*-overexpressing V16D cells were assessed for the expression of terminal NE
360 markers. *HP1α* overexpression significantly promoted the expression of NCAM1 (CD56) and
361 NSE, as shown by both qRT-PCR and Western blotting (Fig. 5B, 5C). *HP1α* overexpression
362 alone was not able to induce NE transdifferentiation (Fig. 5B, 5C). Further transcriptomic
363 analysis of control and *HP1α*-overexpressing V16D cells upon EnZ treatment revealed that
364 *HP1α* overexpression consistently upregulated the expression of a panel of NEPC marker
365 genes and enriched neuronal-associated signaling pathways (Fig. 5D, 5E, S4A). Pearson
366 correlation analyses with transcriptomic data from multiple CRPC clinical cohorts (i.e., the
367 *Beltran et al.* 2016, the *Kumar et al.* 2016, the *Grasso et al.* 2012, and the *Varabally et al.*
368 2005) further demonstrated that high expression of *HP1α* is positively correlated with the

369 expression of terminal NE markers (i.e., *NCAM1*, *NSE*, *CHGA*, *CHGB*) in advanced PCa
370 (10,24,25,27) (Fig. 5F, 5G, S4B, S4C). Overall, these analyses suggest that HP1 α is a
371 potential functional driver promoting NE transdifferentiation.

372

373 **HP1 α represses AR and REST expression and enriches H3K9me3 on their promoters**

374 We further analyzed how HP1 α contributed to the NE phenotype. A major function of
375 HP1 α in heterochromatin is to repress gene expression using epigenetic machineries
376 (31,32), which is an observation supported by our transcriptomic analyses with *HP1 α*
377 knockdown and overexpressing cells (Fig. 5E, S4D). Decreased or loss of expression of the
378 crucial adenocarcinoma lineage-specific transcription factors AR, FOXA1 and REST is a
379 well-established mechanism leading to NE differentiation (12-14). Notably, when *HP1 α* was
380 overexpressed in V16D cells, AR and REST were downregulated at both the mRNA and
381 protein levels (Fig. 6A, 6B, S5A). Consistently, a panel of AR target genes that are
382 repressed in clinical NEPCs are also downregulated upon *HP1 α* overexpression in V16D
383 cells (Fig. 6C). Reciprocally, *HP1 α* knockdown in H660 cells reactivated *AR* and *REST*
384 mRNA expression (Fig. S5B), though their protein levels remained undetectable due to low
385 abundance.

386 We next investigated potential mechanisms underlying the downregulation of AR and
387 REST upon *HP1 α* overexpression. We found that, rather than affecting global
388 heterochromatin related genes, *HP1 α* overexpression significantly enriched (while
389 knockdown impaired) pericentric heterochromatin machineries as determined by GSEA

390 (Fig.6D, S5C-S5E). Pericentric heterochromatin is a constitutive heterochromatin structure
391 characterized by the repressive histone mark H3K9me3 (32). We then performed a
392 chromatin immunoprecipitation (ChIP) assay to examine the occupancy of H3K9me3 on the
393 promoter regions of *AR* and *REST* following *HP1 α* modulation. Interestingly, in V16D cells,
394 *HP1 α* overexpression increased the occupancy of H3K9me3 on both the *AR* and *REST*
395 promoters, while its knockdown in H660 cells decreased H3K9me3 enrichment on the *AR*
396 promoter (Fig. 6E, S5F). In accordance with our findings in cell lines, the pericentric
397 heterochromatin geneset is consistently and significantly enriched in NEPCs compared to
398 adenocarcinomas in our PDX models, multiple clinical cohorts, and GEM models (Fig. 6F,
399 S5G). Meanwhile, Pearson correlation analyses with multiple clinical cohorts showed that
400 *HP1 α* expression is negatively correlated with *AR* and *REST* expression in advanced PCa
401 samples (Fig. 6G, 6H, S5H) (10,24,25,27). Overall, our data indicate that *HP1 α* could
402 regulate expression of the two crucial adenocarcinoma lineage-specific transcription factors
403 *AR* and *REST* potentially via modulating the enrichment of H3K9me3 on their promoters.

404 **DISCUSSION**

405 Loss of luminal epithelial cell characteristics together with gain of small cell
406 neuroendocrine features makes NEPC a completely different disease than typical
407 adenocarcinoma CRPC. This transdifferentiation makes all ARPIs inapplicable despite their
408 otherwise remarkable revolution on the treatment of advanced PCas (1,14). More critically,
409 the application of potent ARPIs for the clinical management of CRPC could accelerate the
410 incidence of NEPC in near future (2,3,33). As such, deciphering the biological and molecular
411 mechanisms underlying NEPC development is fundamentally important for developing novel
412 therapeutics.

413 Gross differences in nuclear hyperchromatic morphology between adenocarcinoma
414 cells and NEPC cells have long been a criterion for NEPC pathological diagnosis. Our study
415 here unmasks, for the first time, the precise molecular basis underlying this NEPC-specific
416 nuclear phenotype and identifies a 36-gene NEPC heterochromatin signature using multiple
417 high-fidelity prostatic adenocarcinoma and NEPC PDXs and two prevalent clinical cohorts.
418 Notably, our heterochromatin gene signature can significantly distinguish NEPCs from
419 adenocarcinomas similar to two other NEPC gene signatures derived from whole-genomic
420 differences, suggesting a crucial function of heterochromatin in NEPC and also a potential
421 application for diagnostic purposes. Furthermore, as epigenetic machineries play a major
422 foundational role in heterochromatin formation and function (6,34), this 36-gene
423 heterochromatin signature also includes 29 epigenetic factors (35). Among them, PcG genes
424 such as *EZH2* have already been demonstrated to play critical roles in NEPC (8,9,36). Thus,

425 these heterochromatin genes also provide a molecular basis for NEPC development and
426 aggressiveness. Considering that the hyperchromatic nuclear pattern in NEPC is also
427 shared by other small cell carcinomas such as small cell lung cancer (SCLC), this
428 heterochromatin signature may be further applicable to small cell carcinomas of other tissue
429 origins (37).

430 From these 36 heterochromatin genes, HP1 α was identified as a potential early
431 driver of NE transdifferentiation. The longitudinal analyses of LTL331 PDX tissues following
432 host castration demonstrated that the upregulated expression of HP1 α is an early event.
433 This is in contrast to a number of genes previously reported to be involved in NEPC
434 development, such as *EZH2*, *CBX2* (9,23), which were only upregulated in the fully
435 developed NEPC LTL331R tumor. Notably, our LTL331/331R model is not only clinically
436 relevant (21,22), but also highly reproducible in delivering the same NE transdifferentiation in
437 18 individual repeats without exception so long as castration is applied. This robust
438 phenomenon indicates that NE transdifferentiation in the LTL331/331R model is lineage
439 determined, and the early changes detected in castrated tumors may thus reflect an
440 inevitable and not stochastic event. More importantly, we indeed demonstrate that HP1 α can
441 promote terminal NE marker expression in adenocarcinoma cells following ADT. In our study,
442 we also noticed that while HP1 α was able to repress AR expression and AR signaling under
443 AR-driven prostatic epithelial status, it cannot function as a neural factor to directly induce
444 the NE phenotype. Only when AR signaling is diminished by ADT can *HP1 α* ectopic
445 expression promote NE transdifferentiation in adenocarcinoma cells. This process both
446 recapitulates the *in vivo* NE transdifferentiation phenotype occurring in the LTL331/331R

447 model, and also mirrors the clinical progression of NEPC where most cases appear after
448 hormonal therapy (3,33). In terminal NEPC cells where HP1 α mainly functions as a regulator
449 of aggressiveness, *HP1 α* knockdown cannot alter NE phenotype (Fig. S6A). Therefore,
450 HP1 α could potentially serve as an early therapeutic target to interfere with disease
451 progression before NEPC fully develops.

452 In addition to being significantly overexpressed in clinical NEPC samples, HP1 α
453 plays a crucial role in terminal NEPC as demonstrated by thorough functional studies in the
454 *bona fide* NEPC cell line NCI-H660. While previous studies have reported the function of
455 HP1 α in breast cancer, lung cancer, and cholangiocarcinoma, its function in prostate cancer
456 remains elusive (38-42). Our data demonstrates that *HP1 α* knockdown in NEPC cells
457 dramatically inhibited proliferation, completely ablated colony formation, and induced
458 apoptotic cell death. Consequently, *HP1 α* depletion markedly inhibited NEPC tumor growth
459 *in vivo*. Alternatively, in V16D adenocarcinoma cells where *HP1 α* overexpression promoted
460 NE transdifferentiation, *HP1 α* overexpression did not significantly enhance proliferation (Fig.
461 S6B). These data suggests that HP1 α is particularly essential for NEPC malignancy, with
462 one potential mechanism being *HP1 α* depletion impairs mitotic machineries. While reported
463 to drive and maintain heterochromatin structure (31,32,43), HP1 α is prominently associated
464 with constitutive heterochromatins (44) as demonstrated through our study. Depletion of
465 *HP1 α* did not affect heterochromatin-related genes universally, but significantly impaired the
466 pericentric constitutive heterochromatin machineries. Pericentric heterochromatin is a key
467 element ensuring proper chromosome segregation in metaphase (6), which is also a major
468 previously reported function of HP1 α (38,45). The abnormally enriched pericentric

469 heterochromatin genes in NEPCs may also explain the highly proliferative feature of NEPC,
470 for which HP1 α may play a driver function. Another potential mechanism underlying the
471 essential function of HP1 α in NEPC aggressiveness is that *HP1 α* depletion impaired DNA
472 damage response (DDR) machineries, which is in accordance with previous studies (46,47).
473 Most recently, another study also reported that a DDR pathway is enriched in NEPC,
474 contributing to NEPC cell proliferation (48). Overall, HP1 α could potentially serve as a
475 therapeutic target for effective management of developed NEPC.

476 Our findings also suggest a novel, HP1 α -mediated mechanism of NEPC
477 development. AR, FOXA1 and REST are the three crucial adenocarcinoma lineage-specific
478 transcription factors maintaining luminal epithelial characteristics (12-14). Our data
479 demonstrates that HP1 α can repress AR and REST expression in adenocarcinoma cells,
480 while its depletion in NEPC cell can reactivate their expression. *HP1 α* gene was first
481 identified to be a modulator of position effect variegation where euchromatic genes
482 abnormally juxtaposed with pericentric heterochromatin could be silenced due to compaction
483 into heterochromatin (49). In our study, we also found that HP1 α may play an epistatic role
484 in regulating the pericentric heterochromatin apparatus. The repressive histone mark
485 H3K9me3 is a hallmark of pericentric heterochromatin and also a major substrate
486 recognized by HP1 α (31,32). Given that the *AR* and *REST* genes are natively located in the
487 vicinity of pericentric heterochromatins (Xq12 and 4q12 respectively, Fig. S6C), they could
488 potentially be sensitive to pericentric heterochromatin deregulation. Our data indeed showed
489 that modulation of *HP1 α* regulates the enrichment of H3K9me3 on the promoters of *AR* and
490 *REST*. Considering the significant enrichment of H3K9me3-characterized pericentric

491 heterochromatin genes in multiple NEPC models and clinical cohorts, our study suggests
492 that the HP1 α /H3K9me3 axis may partially explain the absence or loss of AR and REST
493 expression in NEPCs. Further investigation on genome-wide occupancy of HP1 α and
494 H3K9me3 will provide valuable insights. HP1 α mediates gene silencing together with other
495 precise epigenetic machineries (31). Previous studies have shown that AR expression can
496 also be repressed by the EZH2/H3K27me3 axis (8,36). As such, HP1 α /H3K9me3 might
497 coordinate with EZH2/H3K27me3, establishing the complete repression of AR in NEPCs.
498 Alternative splicing has been suggested to suppress REST in NEPCs (16). HP1 α was also
499 reported to mediate mRNA alternative splicing and exon recognition (50). As such, HP1 α
500 might be involved in mediating REST splicing as well. Our data here suggests
501 HP1 α /H3K9me3 as a new mechanism leading to the silencing of REST mRNA in most
502 NEPC samples.

503 In summary, our data imply a novel mechanism underlying NEPC development:
504 HP1 α drives the abnormal formation of pericentric heterochromatin, which in turn promotes
505 ADT-induced NE transdifferentiation via repressing AR and REST expression, and confers
506 the malignant NEPC phenotype via promoting aggressive proliferation and cell survival.
507 Taken together HP1 α can be considered an early and master mediator of NEPC
508 development and aggressiveness, making it an exceptional novel therapeutic target for
509 potentially effective treatment of NEPC.

510 **ACKNOWLEDGEMENTS**

511 We would like to thank all members of Y.Z.Wang laboratory for technical support and
512 helpful discussions. We also would like to thank Dr. Jin-Tang Dong (Emory University, USA)
513 for providing the plasmids described herein. This work was supported in part by the
514 Canadian Institutes of Health Research (Y.Z.Wang), Terry Fox Research Institute (Y.Z.Wang,
515 ME. Gleave, C.Collins, C.Ong), BC Cancer Foundation (Y.Z.Wang), Urology Foundation
516 (Y.Z.Wang), and Prostate Cancer Canada (Y.Z.Wang). X.Ci was supported by Prostate
517 Cancer Canada-Movember training award. J.Hao and S.Qu were supported by Mitacs
518 Accelerate award. S.Choi was supported by the CIHR Doctoral award.

519 REFERENCES

- 520 1. Attard G, Parker C, Eeles RA, Schroder F, Tomlins SA, Tannock I, *et al.* Prostate
521 cancer. *Lancet* **2016**;387(10013):70-82 doi 10.1016/S0140-6736(14)61947-4.
- 522 2. Eric Jay S, Rahul Raj A, Jiaoti H, Artem S, Li Z, Joshi JA, *et al.* Clinical and genomic
523 characterization of metastatic small cell/neuroendocrine prostate cancer (SCNC) and
524 intermediate atypical prostate cancer (IAC): Results from the SU2C/PCF/AACRWest
525 Coast Prostate Cancer Dream Team (WCDT). *Journal of Clinical Oncology*
526 **2016**;34(15_suppl):5019- doi 10.1200/JCO.2016.34.15_suppl.5019 %U
527 http://ascopubs.org/doi/abs/10.1200/JCO.2016.34.15_suppl.5019.
- 528 3. Vlachostergios PJ, Puca L, Beltran H. Emerging Variants of Castration-Resistant
529 Prostate Cancer. *Curr Oncol Rep* **2017**;19(5):32 doi 10.1007/s11912-017-0593-6.
- 530 4. Humphrey PA. Diagnosis of adenocarcinoma in prostate needle biopsy tissue. *J Clin*
531 *Pathol* **2007**;60(1):35-42 doi 10.1136/jcp.2005.036442.
- 532 5. Fischer AH, Jacobson KA, Rose J, Zeller R. Hematoxylin and eosin staining of tissue
533 and cell sections. *CSH Protoc* **2008**;2008:pdb prot4986 doi 10.1101/pdb.prot4986.
- 534 6. Saksouk N, Simboeck E, Dejardin J. Constitutive heterochromatin formation and
535 transcription in mammals. *Epigenetics Chromatin* **2015**;8:3 doi 10.1186/1756-8935-8-
536 3.
- 537 7. Morgan MA, Shilatifard A. Chromatin signatures of cancer. *Genes Dev*
538 **2015**;29(3):238-49 doi 10.1101/gad.255182.114.
- 539 8. Dardenne E, Beltran H, Benelli M, Gayvert K, Berger A, Puca L, *et al.* N-Myc Induces
540 an EZH2-Mediated Transcriptional Program Driving Neuroendocrine Prostate Cancer.
541 *Cancer Cell* **2016**;30(4):563-77 doi 10.1016/j.ccell.2016.09.005.
- 542 9. Clermont PL, Lin D, Crea F, Wu R, Xue H, Wang Y, *et al.* Polycomb-mediated
543 silencing in neuroendocrine prostate cancer. *Clinical epigenetics* **2015**;7(1):40 doi
544 10.1186/s13148-015-0074-4.
- 545 10. Beltran H, Prandi D, Mosquera JM, Benelli M, Puca L, Cyrta J, *et al.* Divergent clonal
546 evolution of castration-resistant neuroendocrine prostate cancer. *Nat Med* **2016** doi
547 10.1038/nm.4045.
- 548 11. Ku SY, Rosario S, Wang Y, Mu P, Seshadri M, Goodrich ZW, *et al.* Rb1 and Trp53
549 cooperate to suppress prostate cancer lineage plasticity, metastasis, and
550 antiandrogen resistance. *Science* **2017**;355(6320):78-83 doi
551 10.1126/science.aah4199.
- 552 12. Wright ME, Tsai MJ, Aebersold R. Androgen receptor represses the neuroendocrine
553 transdifferentiation process in prostate cancer cells. *Mol Endocrinol* **2003**;17(9):1726-
554 37 doi 10.1210/me.2003-0031.
- 555 13. Lapuk AV, Wu C, Wyatt AW, McPherson A, McConeghy BJ, Brahmabhatt S, *et al.*
556 From sequence to molecular pathology, and a mechanism driving the
557 neuroendocrine phenotype in prostate cancer. *J Pathol* **2012**;227(3):286-97 doi
558 10.1002/path.4047.
- 559 14. Terry S, Beltran H. The many faces of neuroendocrine differentiation in prostate
560 cancer progression. *Front Oncol* **2014**;4:60 doi 10.3389/fonc.2014.00060.

- 561 15. Kim J, Jin H, Zhao JC, Yang YA, Li Y, Yang X, *et al.* FOXA1 inhibits prostate cancer
562 neuroendocrine differentiation. *Oncogene* **2017**;36(28):4072-80 doi
563 10.1038/onc.2017.50.
- 564 16. Li Y, Donmez N, Sahinalp C, Xie N, Wang Y, Xue H, *et al.* SRRM4 Drives
565 Neuroendocrine Transdifferentiation of Prostate Adenocarcinoma Under Androgen
566 Receptor Pathway Inhibition. *Eur Urol* **2016** doi 10.1016/j.eururo.2016.04.028.
- 567 17. Zou M, Toivanen R, Mitrofanova A, Floc'h N, Hayati S, Sun Y, *et al.*
568 Transdifferentiation as a Mechanism of Treatment Resistance in a Mouse Model of
569 Castration-resistant Prostate Cancer. *Cancer discovery* **2017** doi 10.1158/2159-
570 8290.CD-16-1174.
- 571 18. Lee John K, Phillips John W, Smith Bryan A, Park Jung W, Stoyanova T, McCaffrey
572 Erin F, *et al.* N-Myc Drives Neuroendocrine Prostate Cancer Initiated from Human
573 Prostate Epithelial Cells. *Cancer Cell* **2016** doi 10.1016/j.ccell.2016.03.001.
- 574 19. Mu P, Zhang Z, Benelli M, Karthaus WR, Hoover E, Chen CC, *et al.* SOX2 promotes
575 lineage plasticity and antiandrogen resistance in TP53- and RB1-deficient prostate
576 cancer. *Science* **2017**;355(6320):84-8 doi 10.1126/science.aah4307.
- 577 20. Bishop JL, Thaper D, Vahid S, Davies A, Ketola K, Kuruma H, *et al.* The Master
578 Neural Transcription Factor BRN2 is an Androgen Receptor Suppressed Driver of
579 Neuroendocrine Differentiation in Prostate Cancer. *Cancer discovery* **2016** doi
580 10.1158/2159-8290.CD-15-1263.
- 581 21. Lin D, Wyatt AW, Xue H, Wang Y, Dong X, Haegert A, *et al.* High fidelity patient-
582 derived xenografts for accelerating prostate cancer discovery and drug development.
583 *Cancer Res* **2014**;74(4):1272-83 doi 10.1158/0008-5472.CAN-13-2921-T.
- 584 22. Akamatsu S, Wyatt AW, Lin D, Lysakowski S, Zhang F, Kim S, *et al.* The Placental
585 Gene PEG10 Promotes Progression of Neuroendocrine Prostate Cancer. *Cell*
586 *reports* **2015**;12(6):922-36 doi 10.1016/j.celrep.2015.07.012.
- 587 23. Beltran H, Rickman DS, Park K, Chae SS, Sboner A, MacDonald TY, *et al.* Molecular
588 characterization of neuroendocrine prostate cancer and identification of new drug
589 targets. *Cancer discovery* **2011**;1(6):487-95 doi 10.1158/2159-8290.CD-11-0130.
- 590 24. Grasso CS, Wu YM, Robinson DR, Cao X, Dhanasekaran SM, Khan AP, *et al.* The
591 mutational landscape of lethal castration-resistant prostate cancer. *Nature*
592 **2012**;487(7406):239-43 doi 10.1038/nature11125.
- 593 25. Kumar A, Coleman I, Morrissey C, Zhang X, True LD, Gulati R, *et al.* Substantial
594 interindividual and limited intraindividual genomic diversity among tumors from men
595 with metastatic prostate cancer. *Nat Med* **2016** doi 10.1038/nm.4053.
- 596 26. Cerami E, Gao J, Dogrusoz U, Gross BE, Sumer SO, Aksoy BA, *et al.* The cBio
597 cancer genomics portal: an open platform for exploring multidimensional cancer
598 genomics data. *Cancer discovery* **2012**;2(5):401-4 doi 10.1158/2159-8290.CD-12-
599 0095.
- 600 27. Varambally S, Yu J, Laxman B, Rhodes DR, Mehra R, Tomlins SA, *et al.* Integrative
601 genomic and proteomic analysis of prostate cancer reveals signatures of metastatic
602 progression. *Cancer Cell* **2005**;8(5):393-406 doi 10.1016/j.ccr.2005.10.001.
- 603 28. Subramanian A, Tamayo P, Mootha VK, Mukherjee S, Ebert BL, Gillette MA, *et al.*
604 Gene set enrichment analysis: a knowledge-based approach for interpreting

- 605 genome-wide expression profiles. *Proc Natl Acad Sci U S A* **2005**;102(43):15545-50
606 doi 10.1073/pnas.0506580102.
- 607 29. Liberzon A, Subramanian A, Pinchback R, Thorvaldsdottir H, Tamayo P, Mesirov JP.
608 Molecular signatures database (MSigDB) 3.0. *Bioinformatics* **2011**;27(12):1739-40
609 doi 10.1093/bioinformatics/btr260.
- 610 30. Johnson BE, Whang-Peng J, Naylor SL, Zbar B, Brauch H, Lee E, *et al.* Retention of
611 chromosome 3 in extrapulmonary small cell cancer shown by molecular and
612 cytogenetic studies. *J Natl Cancer Inst* **1989**;81(16):1223-8.
- 613 31. Eissenberg JC, Elgin SC. HP1a: a structural chromosomal protein regulating
614 transcription. *Trends Genet* **2014**;30(3):103-10 doi 10.1016/j.tig.2014.01.002.
- 615 32. Maison C, Almouzni G. HP1 and the dynamics of heterochromatin maintenance.
616 *Nature reviews Molecular cell biology* **2004**;5(4):296-304 doi 10.1038/nrm1355.
- 617 33. Rickman DS, Beltran H, Demichelis F, Rubin MA. Biology and evolution of poorly
618 differentiated neuroendocrine tumors. *Nat Med* **2017**;23(6):1-10 doi 10.1038/nm.4341.
- 619 34. Grewal SI, Jia S. Heterochromatin revisited. *Nat Rev Genet* **2007**;8(1):35-46 doi
620 10.1038/nrg2008.
- 621 35. Medvedeva YA, Lennartsson A, Ehsani R, Kulakovskiy IV, Vorontsov IE,
622 Panahandeh P, *et al.* EpiFactors: a comprehensive database of human epigenetic
623 factors and complexes. *Database (Oxford)* **2015**;2015:bav067 doi
624 10.1093/database/bav067.
- 625 36. Kleb B, Estecio MR, Zhang J, Tzelepi V, Chung W, Jelinek J, *et al.* Differentially
626 methylated genes and androgen receptor re-expression in small cell prostate
627 carcinomas. *Epigenetics* **2016**:0 doi 10.1080/15592294.2016.1146851.
- 628 37. Travis WD. Update on small cell carcinoma and its differentiation from squamous cell
629 carcinoma and other non-small cell carcinomas. *Mod Pathol* **2012**;25 Suppl 1:S18-30
630 doi 10.1038/modpathol.2011.150.
- 631 38. De Koning L, Savignoni A, Boumendil C, Rehman H, Asselain B, Sastre-Garau X, *et al.*
632 Heterochromatin protein 1alpha: a hallmark of cell proliferation relevant to clinical
633 oncology. *EMBO Mol Med* **2009**;1(3):178-91 doi 10.1002/emmm.200900022.
- 634 39. Cheng W, Tian L, Wang B, Qi Y, Huang W, Li H, *et al.* Downregulation of HP1alpha
635 suppresses proliferation of cholangiocarcinoma by restoring SFRP1 expression.
636 *Oncotarget* **2016**;7(30):48107-19 doi 10.18632/oncotarget.10371.
- 637 40. Yu YH, Chiou GY, Huang PI, Lo WL, Wang CY, Lu KH, *et al.* Network biology of
638 tumor stem-like cells identified a regulatory role of CBX5 in lung cancer. *Scientific*
639 *reports* **2012**;2:584 doi 10.1038/srep00584.
- 640 41. Itsumi M, Shiota M, Yokomizo A, Kashiwagi E, Takeuchi A, Tatsugami K, *et al.*
641 Human heterochromatin protein 1 isoforms regulate androgen receptor signaling in
642 prostate cancer. *Journal of molecular endocrinology* **2013**;50(3):401-9.
- 643 42. Shapiro E, Huang H, Ruoff R, Lee P, Tanese N, Logan SK. The heterochromatin
644 protein 1 family is regulated in prostate development and cancer. *J Urol*
645 **2008**;179(6):2435-9 doi 10.1016/j.juro.2008.01.091.
- 646 43. Larson AG, Elnatan D, Keenen MM, Trnka MJ, Johnston JB, Burlingame AL, *et al.*
647 Liquid droplet formation by HP1alpha suggests a role for phase separation in
648 heterochromatin. *Nature* **2017** doi 10.1038/nature22822.

- 649 44. Nielsen AL, Ortiz JA, You J, Oulad-Abdelghani M, Khechumian R, Gansmuller A, *et al.* Interaction with members of the heterochromatin protein 1 (HP1) family and
650 *al.* Interaction with members of the heterochromatin protein 1 (HP1) family and
651 histone deacetylation are differentially involved in transcriptional silencing by
652 members of the TIF1 family. *EMBO J* **1999**;18(22):6385-95 doi
653 10.1093/emboj/18.22.6385.
- 654 45. Abe Y, Sako K, Takagaki K, Hirayama Y, Uchida KS, Herman JA, *et al.* HP1-Assisted
655 Aurora B Kinase Activity Prevents Chromosome Segregation Errors. *Dev Cell*
656 **2016**;36(5):487-97 doi 10.1016/j.devcel.2016.02.008.
- 657 46. Luijsterburg MS, Dinant C, Lans H, Stap J, Wiernasz E, Lagerwerf S, *et al.*
658 Heterochromatin protein 1 is recruited to various types of DNA damage. *J Cell Biol*
659 **2009**;185(4):577-86 doi 10.1083/jcb.200810035.
- 660 47. Lee YH, Kuo CY, Stark JM, Shih HM, Ann DK. HP1 promotes tumor suppressor
661 BRCA1 functions during the DNA damage response. *Nucleic Acids Res*
662 **2013**;41(11):5784-98 doi 10.1093/nar/gkt231.
- 663 48. Zhang W, Liu B, Wu W, Li L, Broom BM, Basourakos SM, *et al.* Targeting the MYCN-
664 PARP-DNA Damage Response Pathway in Neuroendocrine Prostate Cancer. *Clin*
665 *Cancer Res* **2017** doi 10.1158/1078-0432.CCR-17-1872.
- 666 49. Eissenberg JC, James TC, Foster-Hartnett DM, Hartnett T, Ngan V, Elgin SC.
667 Mutation in a heterochromatin-specific chromosomal protein is associated with
668 suppression of position-effect variegation in *Drosophila melanogaster*. *Proc Natl*
669 *Acad Sci U S A* **1990**;87(24):9923-7.
- 670 50. Yearim A, Gelfman S, Shayevitch R, Melcer S, Glaich O, Mallm JP, *et al.* HP1 is
671 involved in regulating the global impact of DNA methylation on alternative splicing.
672 *Cell reports* **2015**;10(7):1122-34 doi 10.1016/j.celrep.2015.01.038.

673

674 **FIGURE LEGENDS**

675 **Figure 1. NEPC has a distinctive heterochromatin gene signature.** (A-F) GSEA show the
676 enrichment of heterochromatin-associated genes in NEPC from (A) PDX models, (B) the
677 *Beltran et al.* 2011 cohort (23), (C) the *Beltran et al.* 2016 cohort (10), and in NE-like GEM
678 models derived from (D) *Rb/Trp53* DKO or *Pten/Rb/Trp53* TKO (11), (E) *Npp53* CRPC with
679 NE differentiation (17), (F) and *Nmyc* overexpression (8). “NES” stands for normalized
680 enrichment score; FDR q values were calculated using 1000 gene permutations except for
681 (C), where Gsea preranked was applied. (G) Heatmap showing the hierarchical clustering
682 among all PDX samples suggests a unique upregulation of heterochromatin signature genes
683 in NEPC PDX tumors. (H) Weighted NE scores and heterochromatin scores of
684 adenocarcinoma and NEPC PDX tumors and two clinical cohorts. NE scores were
685 calculated based on the gene panels from *Beltran et al.* 2016 (10) and *Lee et al.* 2016 (18).
686 Heterochromatin scores were calculated based on the weighted gene panel from (G).
687 Scatter plots show the calculated score of each tumor sample, with lines indicating the mean
688 value and 95% CI. The *p*-values were calculated using the unpaired two-tail Student’s *t*-test.
689 See also Fig. S1.

690 **Figure 2. HP1 α expression is upregulated during NE transdifferentiation and in NEPC**
691 **PDX models.** (A) A heatmap showing the gene expression changes in the LTL331/331R NE
692 transdifferentiation PDX model. Heterochromatin signature genes, AR signaling targets, and
693 NE markers are included. RNA-seq data from two individual samples at each time point was
694 used (pre: LTL331 pre-castration; Cx: 8 weeks post-castration; Rep: LTL331R NEPC

695 relapse). Average differences in expression between castrated and pre-castrated tumors (C
696 vs. P) are shown in a separate heatmap. (B-D) HP1 α expression in PDX models, as
697 determined by (B) qRT-PCR, (C) IHC, and (D) Western blotting. Scatter plots show relative
698 mRNA expression or IHC score for each sample, with lines indicating median values. (E-G)
699 HP1 α expression in the LTL331/331R castration-induced NE transdifferentiation PDX model,
700 as determined by (E) qRT-PCR, (F) Western blotting, and (G) IHC. Data show mean \pm SEM
701 from three replicates. The p -values (B, C, E) were calculated with unpaired two-tail Student's
702 t -tests. See also Fig. S2.

703 **Figure 3. HP1 α expression is upregulated in clinical NEPC samples and correlates**
704 **with poor prognosis in adenocarcinomas.** (A-C) *HP1 α* mRNA expression in NEPC vs.
705 adenocarcinoma from (A) the *Beltran, et al.* 2011 cohort (23), (B) the *Beltran, et al.* 2016
706 cohort (10), and (C) the *Grasso, et al.* 2012 cohort (24). Scatter plots show RNA expression
707 data of each sample, with lines indicating median values. The p -values were calculated
708 using unpaired two-tail Student's t -test. (D) Staining intensity for the HP1 α protein in primary
709 adenocarcinomas (n=103), CRPC-adenocarcinomas (n=120), and NEPC (n=8) as
710 determined by IHC of the VPC TMA. Box plots show the mean with whiskers representing 5-
711 95% percentile values. The p -values were calculated using unpaired two-tail Student's t -test.
712 (E) Representative IHC images for the various staining intensities (0 to 3) are shown, with
713 the lower panels being magnifications of the selected regions in the upper panels. Scale
714 bars in the upper and lower panels represent 100 μ m and 10 μ m respectively. (F-G) Kaplan-
715 Meier survival analyses of estimated (F) relapse-free survival time based on the HP1 α IHC
716 score of primary adenocarcinomas from the VPC cohort with follow-up information (n=37)

717 and (G) prostate-cancer specific survival time after first hormonal therapy based on *HP1α*
718 mRNA from metastatic adenocarcinomas in the Grasso, *et al.* 2012 cohort (n=33) (24). The
719 *p*-values were calculated using the log-rank test to determine the difference in outcomes
720 between patients with high (red) and low (black) *HP1α* expression.

721 **Figure 4. *HP1α* is essential for the aggressive growth of NEPC cells and tumors.** (A)

722 Stable knockdown of *HP1α* in NCI-H660 cells by lentiviral transduction. Changes to *HP1α*
723 mRNA and protein levels were determined by qRT-PCR and Western blotting respectively.
724 Bar graph shows mean \pm SEM. The *p*-value was calculated by unpaired two-tail Student's *t*-
725 test. (B) Cell growth assay of *HP1α* knockdown H660 cells as determined by crystal violet
726 staining. Stable cells were plated in four replicate wells for each time point and cell numbers
727 were determined based on the absorbance at O.D. 572 nm of crystal violet dissolved in 2%
728 SDS. Data is graphed as mean \pm SEM. Representative images demonstrating cell numbers
729 at the final time point are shown. The *p*-value was calculated by two-way ANOVA. (C)
730 Colony formation assay of *HP1α* knockdown H660 cells as determined by crystal violet
731 staining. Cells were plated in four replicate wells for each stable line and colony numbers
732 were counted manually. Bar graph shows mean \pm SEM. Representative images
733 demonstrating colony numbers are shown. The *p*-value was calculated by unpaired two-tail
734 Student's *t*-test. (D) An EdU incorporation assay was performed by incubating stable *HP1α*
735 knockdown H660 cells with 10 μ M EdU for 4 hours. EdU-labeled cells (red) and total cells
736 counterstained with DAPI (blue) were counted for at least 10 fields. Bar graph shows the
737 mean (EdU-positive ratio) \pm SEM. Representative images are shown with the scale bar
738 representing 100 μ m. The *p*-values were calculated by unpaired two-tail Student's *t*-test. (E)

739 An apoptosis assay measuring caspase-3 activity using the ApoLive-Glo™ Multiplex
740 Reagent. Relative apoptosis was determined by the ratio of luminescence (caspase-3
741 activity) to fluorescence (AFC signal for viable cells). Bar graph shows mean \pm SEM
742 (normalized to shC). The *p*-values were calculated by unpaired two-tail Student's *t*-test. (F)
743 Cell death following stable *HP1 α* knockdown in H660 cells was determined by flow
744 cytometry with 7-AAD staining. 10,000 single cells were collected for analysis with dead cells
745 being 7-AAD positive. Bar graph shows mean \pm SEM (normalized to shC). The *p*-values
746 were calculated by unpaired two-tail Student's *t*-test. (G) Apoptosis markers cleaved-
747 caspase 3 and cleaved-PARP1 as determined by Western blotting following stable *HP1 α*
748 knockdown in H660 cells. Intact caspase 3 and PARP1 serve as controls. CI stands for
749 "cleaved". (H) Selected gene sets enriched in *HP1 α* - versus *control*- knockdown H660 cells
750 as analyzed by GSEA. The x-axis represents normalized enrichment score (NES). FDR of all
751 gene sets is less than 0.05 calculated by 1000 permutations. (I-J) Stable H660 cell lines shC
752 and KD2 were each grafted into four NSG mice (eight tumors total) to assess *in vivo*
753 xenograft tumor growth. (I) Tumor volume was measured starting from when palpable tumor
754 appears to when mice were euthanized. Line graph shows mean \pm SEM, with *p*-value
755 calculated by two-way ANOVA. Tumor images are shown in the right panel. (J) Fresh tumors
756 were also weighed at sample collection. Bar graph shows mean \pm SEM with The *p*-value
757 was calculated by unpaired two-tail Student's *t*-test. See also Fig. S3.

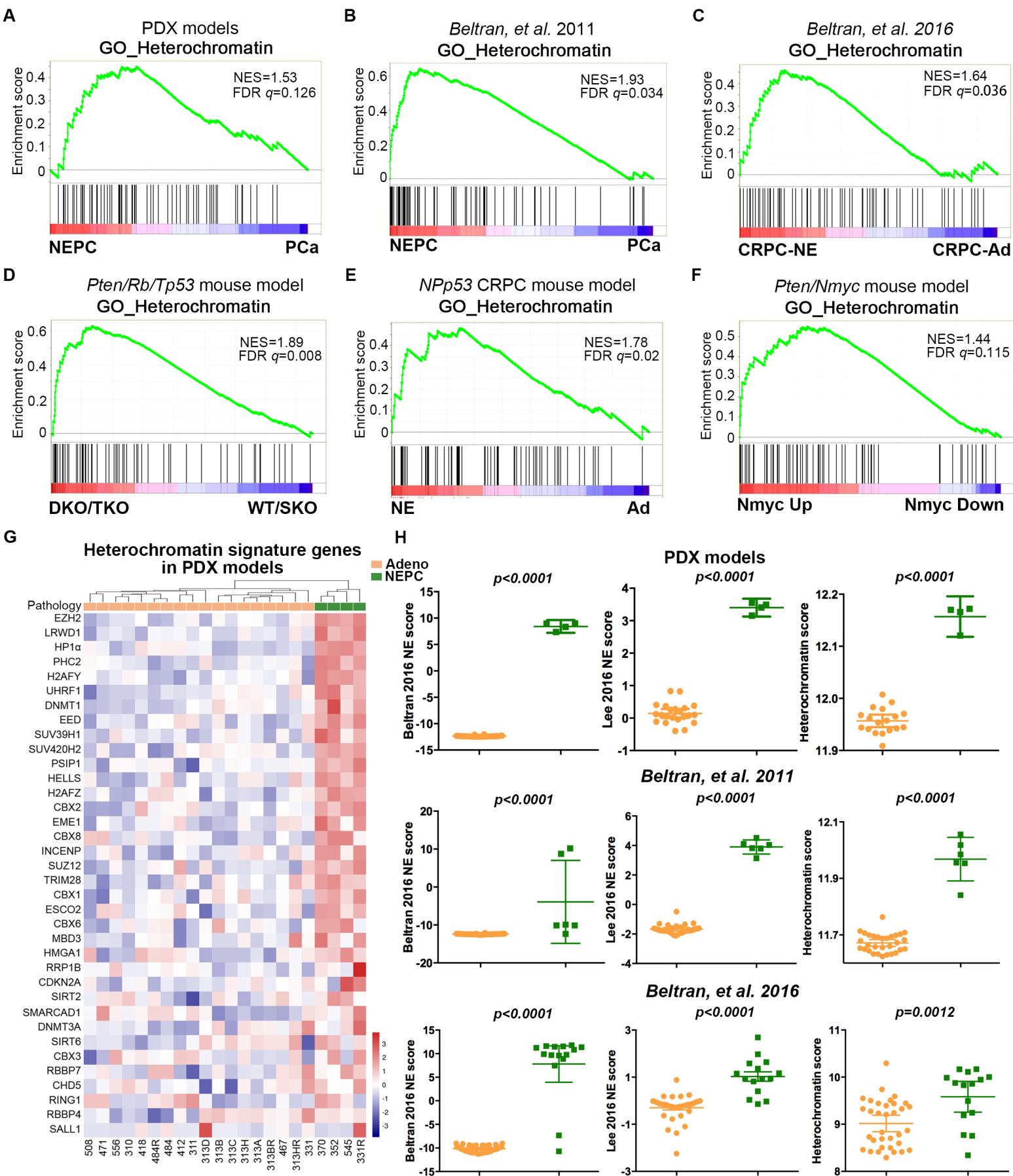
758 **Figure 5. *HP1 α* promotes NE transdifferentiation of prostatic adenocarcinoma cells**

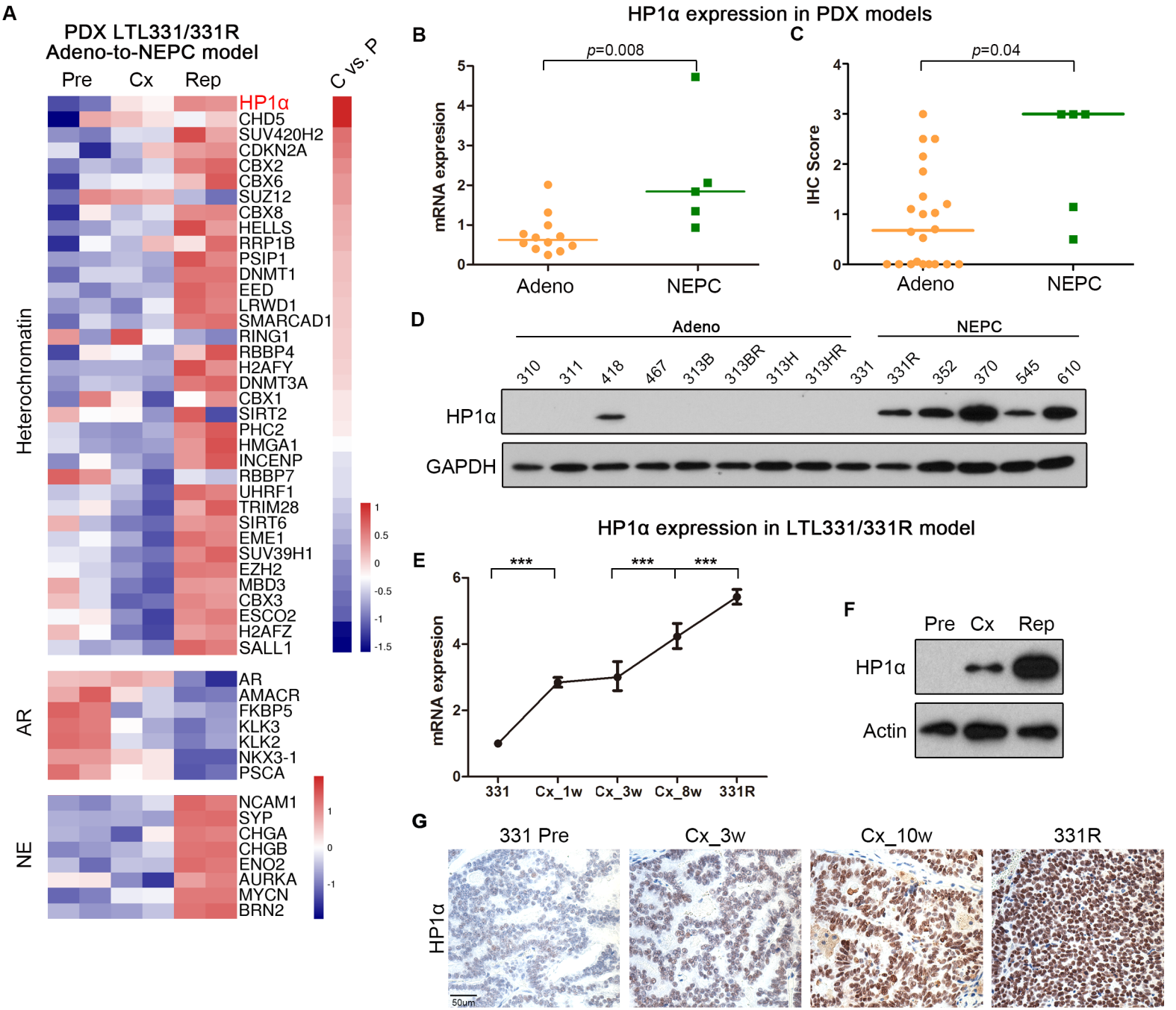
759 **following ADT.** (A) Ectopic expression of *HP1 α* in LNCaP-V16D cells as determined by
760 Western blotting. (B-C) Induction of NE transdifferentiation with ADT in V16D cells stably

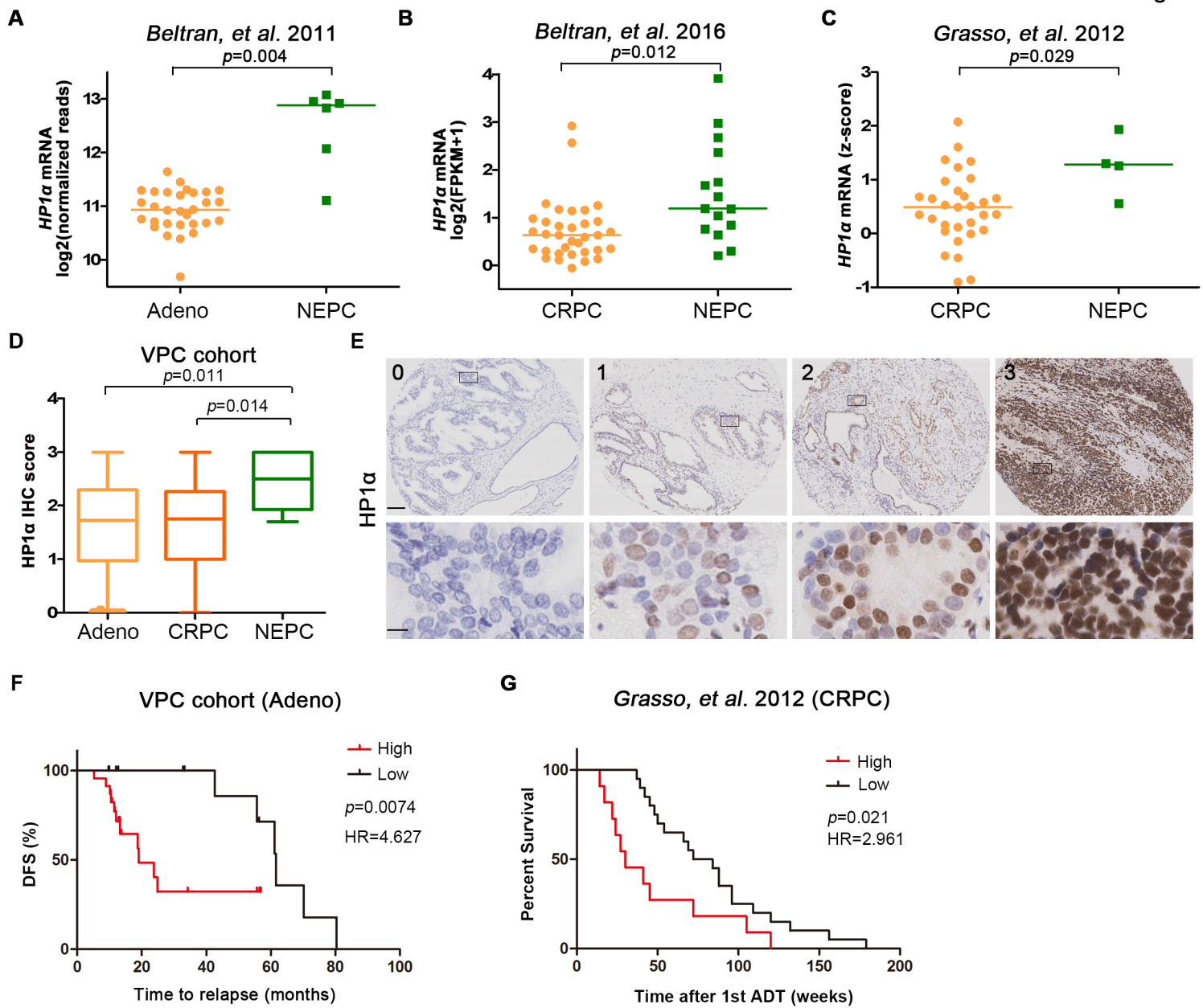
761 overexpressing *HP1α*. Relative mRNA and protein expression of terminal NE markers (SYP,
762 CHGA, NSE, NCAM1) were detected by (B) qRT-PCR and (C) Western blotting in stable
763 cells cultured in complete medium (FBS), CSS, and CSS with 10 μM EnZ 14 days. Bar
764 graphs show mean ± SEM. The *p*-values were calculated by unpaired two-tail Student's *t*-
765 tests comparing *HP1α*- to control- overexpressing cells. Relative band intensities as
766 determined by ImageJ are indicated, with actin serving as internal control. (D) A heatmap
767 comparing expression of NEPC marker genes in the indicated V16D cells upon EnZ
768 treatment. The select NEPC marker genes upregulated by *HP1α* overexpression are
769 similarly upregulated in clinical NEPCs in the *Beltran, et al.* 2011 cohort (23). (E) Top 10
770 pathways significantly enriched in *HP1α* overexpressing V16D cells compared to control
771 cells as analyzed with IPA. (F-G) Pearson correlation analysis of *HP1α* mRNA expression
772 and the expression of various NE markers in advanced PCa samples. (F) Correlation with
773 *NCAM1* and *NSE* expression in the *Beltran, et al.* 2016 cohort (10), and (G) correlation with
774 *CHGB* and *CHGA* expression in the *Kumar et al.* 2015 cohort (25). See also Fig. S4.

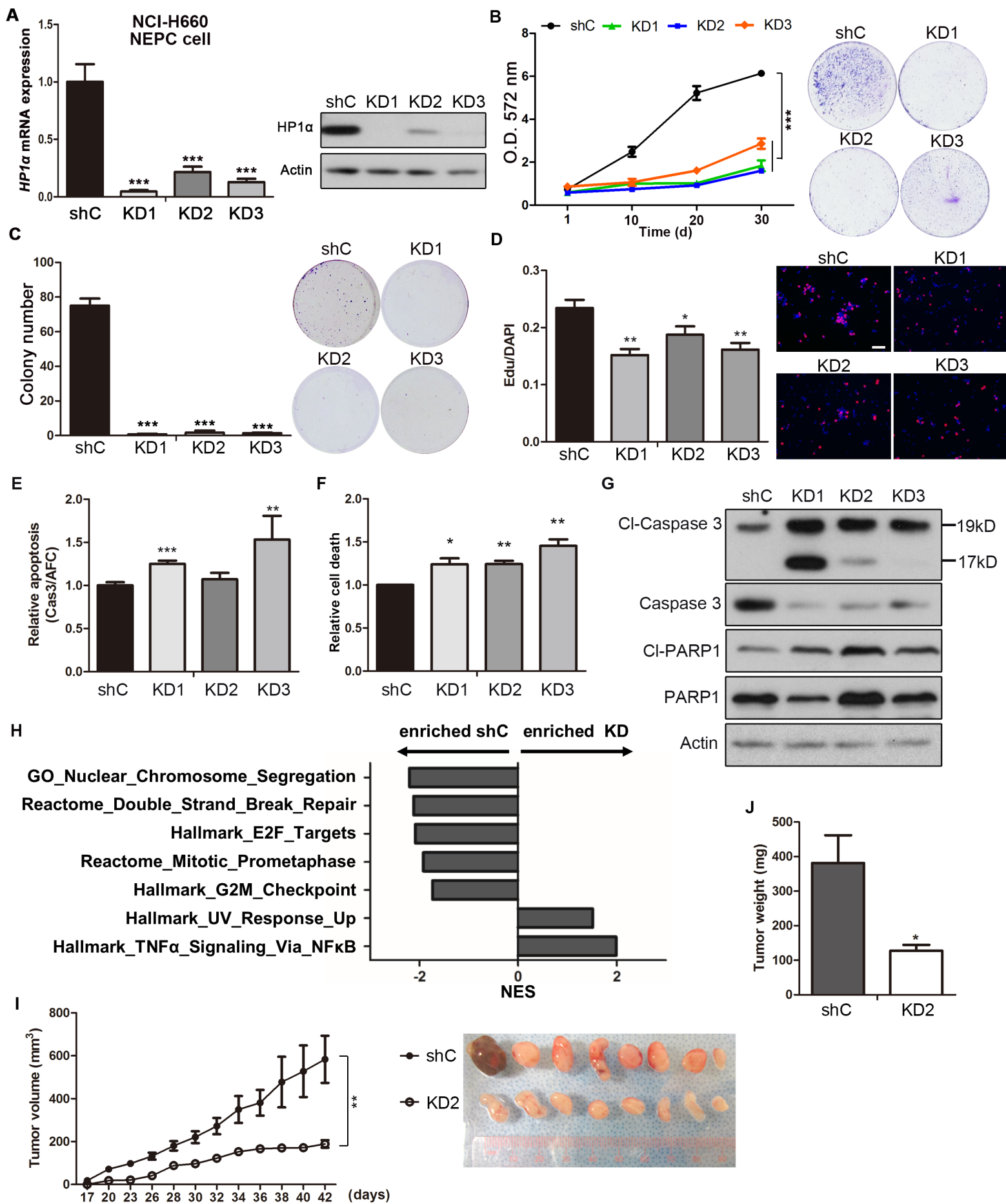
775 **Figure 6. *HP1α* represses AR and REST expression and enriches H3K9me3 on their**
776 **promoters.** (A-B) AR and REST expression in stable V16D cells overexpressing *HP1α* as
777 determined by (A) qRT-PCR and (B) Western blotting. Bar graphs show mean ± SEM. The
778 *p*-values were calculated by unpaired two-tail Student's *t*-test. (C) A heatmap comparing
779 expression of AR signaling genes in the indicated V16D cells. The select AR target genes
780 downregulated by *HP1α* overexpression are similarly downregulated in clinical NEPCs in the
781 *Beltran, et al.* 2011 cohort (23). (D) GSEA of V16D cells with stable *HP1α* overexpression.
782 Expression of pericentric heterochromatin components are upregulated by *HP1α*

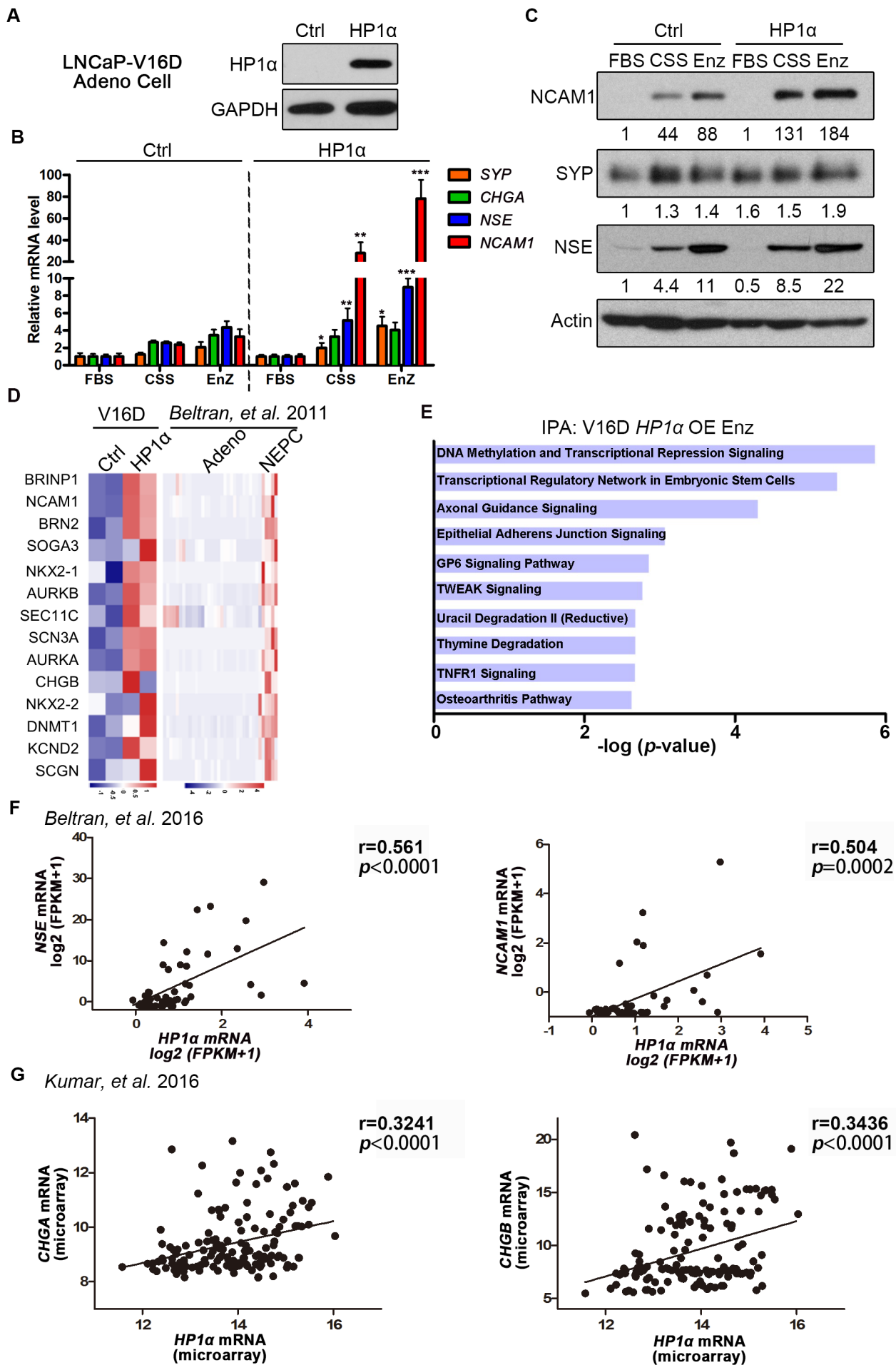
783 overexpression. “NES” stands for normalized enrichment score; FDR q values were
784 calculated using 1000 gene permutations. (E) CHIP-PCR shows the enrichment of H3K9me3
785 on the promoters of *AR* and *REST* in V16D cells with *HP1 α* overexpression, *NC* is a
786 negative control region. Bar graphs show mean \pm SEM. The *p*-values were calculated by
787 unpaired two-tail Student’s *t*-test. (F) GSEA show the enrichment of pericentric
788 heterochromatin genes in human NEPC samples and mouse NE-like tumors. The y-axis
789 represents normalized enrichment score (NES) and the x-axis denotes clinical cohorts and
790 GEM models. FDR is less than 0.15 calculated by 1000 permutations. (G-H) Pearson
791 correlation analysis of *HP1 α* mRNA expression and *AR* and *REST* mRNA levels from (G)
792 the *Beltran et al.* 2016 (10) and (H) the *Kumar et al.* 2016 cohorts (25). See also Fig. S5.

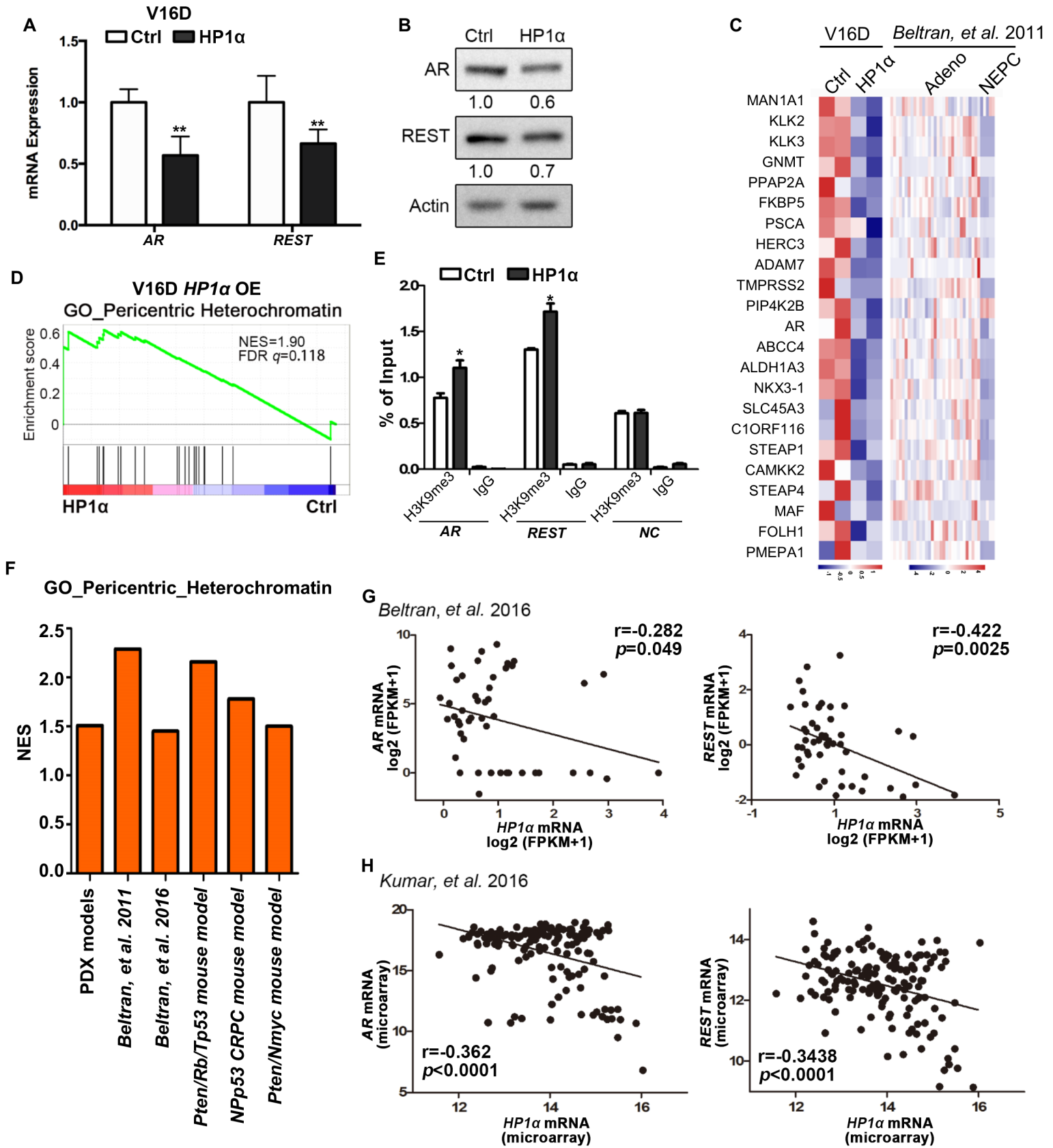












Cancer Research

The Journal of Cancer Research (1916–1930) | The American Journal of Cancer (1931–1940)

Heterochromatin protein 1 α mediates development and aggressiveness of neuroendocrine prostate cancer

Xinpei Ci, Jun Hao, Xin Dong, et al.

Cancer Res Published OnlineFirst February 27, 2018.

Updated version	Access the most recent version of this article at: doi: 10.1158/0008-5472.CAN-17-3677
Supplementary Material	Access the most recent supplemental material at: http://cancerres.aacrjournals.org/content/suppl/2018/02/27/0008-5472.CAN-17-3677.DC1
Author Manuscript	Author manuscripts have been peer reviewed and accepted for publication but have not yet been edited.

E-mail alerts	Sign up to receive free email-alerts related to this article or journal.
Reprints and Subscriptions	To order reprints of this article or to subscribe to the journal, contact the AACR Publications Department at pubs@aacr.org .
Permissions	To request permission to re-use all or part of this article, use this link http://cancerres.aacrjournals.org/content/early/2018/02/27/0008-5472.CAN-17-3677 . Click on "Request Permissions" which will take you to the Copyright Clearance Center's (CCC) Rightslink site.